

Cite this: *Polym. Chem.*, 2011, **2**, 1174

www.rsc.org/polymers

PAPER

Synthesis and physical gelation induced by self-assembly of well-defined poly(arylene ether sulfone)s with various numbers of arms†

Jeyoung Park, Myungeun Seo,‡ Hyungsam Choi and Sang Youl Kim*

Received 22nd December 2010, Accepted 13th February 2011

DOI: 10.1039/c0py00418a

A series of well-defined poly(arylene ether sulfone)s were synthesized (**1P–4P**) by chain-growth condensation polymerization with amide initiators having various numbers of initiating sites. Differential Scanning Calorimetry (DSC) study of the polymers revealed that branched polymers (**3P** and **4P**) had higher glass transition temperatures (T_g) than linear polymers (**1P** and **2P**) when they had the identical concentration of end groups. However, the viscosity of the polymers decreases as the number of branches increase due to the change of the hydrodynamic volume. Interestingly physical gelation of THF solution of these polymers was observed. Analyses of the self-assembled structure by FE-SEM, FE-TEM, temperature-dependent ^1H NMR, FT-IR, and XRD indicated that the formation of fibrillar network was driven by the hydrogen bonding of aromatic amides.

Introduction

Control of polymer architecture is very important to make polymers with controlled properties.^{1–8} Star-shaped polymers, for example, have a number of arms that are joined at the core and possess different characteristics compared to linear polymers such as smaller hydrodynamic volume and reduced viscosity because of their compact nature.^{9–11} For the synthesis of well-defined star-shaped polymers with a controlled number and length of arms, use of controlled polymerization methods is essential and controlled polymerization with a multifunctional initiator has been used.^{1,9–15} However, most of star-shaped polymers synthesized are aliphatic polymers mainly because controlled condensation polymerization of aromatic polymers has been difficult. A recent development of chain-growth condensation polymerization (CGCP) opens an easy access for well-defined aromatic polymers such as aromatic polyamides and polyethers,^{16,17} and synthesis of star-shaped aromatic polyamides have been demonstrated.^{18,19}

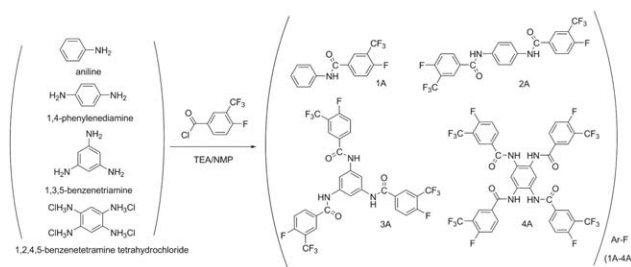
Poly(arylene ether sulfone) (PAES) is one of the well-known high-performance polymers with excellent thermal and mechanical properties,²⁰ but the synthesis of well-defined star-shaped PAES was reported only recently.²¹ In this contribution, we report the first synthesis of well-defined PAES with various

numbers of arms which show that their properties are strongly dependent on the architecture. Interestingly, self-assembly of the well-defined PAESs having amide initiators induced a physical gelation of the THF solution. Only a few examples of thermoreversible gelation induced by star-shaped polymers have been reported.^{22–28} This study introduces a new family of polymers which self-assemble and induce a gelation through hydrogen bonds in the core.

Results and discussion

Synthesis of poly(arylene ether sulfone)s from multi-arm initiators

For the synthesis of well-defined PAESs *via* CGCP, multifunctional initiators with controlled number of initiating sites were necessary. In this study, four kinds of initiators were synthesized by amidation reaction between 4-fluoro-3-trifluoromethylbenzoylchloride and aromatic amines as shown in Scheme 1. The number of initiating sites was simply controlled by using aromatic compounds with a different number of amine



Scheme 1 Synthesis of multi-arm initiators (**1A**, **2A**, **3A**, and **4A**).

Department of Chemistry, Korea Advanced Institute of Science and Technology (KAIST), 373-1, Guseong-dong, Yuseong-gu, Daejeon, 305-701, Korea. E-mail: kimsy@kaist.ac.kr; Fax: +82 42-350-8177; Tel: +82 42-350-2834

† Electronic supplementary information (ESI) available: Experimental details, ^1H NMR and FT-IR spectra of polymers. See DOI: 10.1039/c0py00418a

‡ Current address: Department of Chemistry, University of Minnesota, Minneapolis, MN, 55455-0431, USA.

groups. Because the fluorine groups in the initiators were activated by the amide carbonyl group at *para* position and the trifluoromethyl group at *ortho* position, the initiators were expected to initiate CGCP of the AB type monomer **1**, 4-fluoro-4'-hydroxydiphenyl sulfone potassium salt.

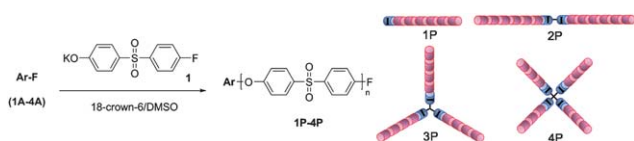
With the synthesized initiators, polymerization of 4-fluoro-4'-hydroxydiphenyl sulfone potassium salt (**1**) was carried out according to the reported procedure for linear PAES²⁹ with some modification (Scheme 2). In a typical run, polymerization was conducted in DMSO with 5 wt% monomer concentration using 18-crown-6 as an additive. The feed ratio of monomer to initiator was varied to control the molecular weight of the polymer, and the reaction temperature was maintained at 100 °C to avoid self-polymerization of the monomer. GPC analysis of the resulting polymers in THF indicates that narrow molecular weight distributions (PDI < 1.3) were obtained in every polymerization, suggesting that polymerization proceeded in a controlled manner (Fig. 1).

The chemical structure of the polymers was analyzed by ¹H NMR spectroscopy, which showed that the proton integration ratio of the initiator moiety to the end group is close to 1 as shown in Fig. 2 and S1 (see ESI†). Also, the number average molecular weights (M_n)s of the polymers were obtained by comparing the integral value of the repeating units (A) and the end group (1). The M_n s obtained by ¹H NMR were smaller than the M_n s measured by GPC. The 4-arm star-shaped polymer (**4P**) has the smallest difference between the M_n s determined by ¹H NMR and GPC analyses, indicating the polymers possess relatively smaller hydrodynamic volume and elute later during the GPC analysis compared to their linear analogues of similar molecular weight. MALDI-TOF mass spectroscopy analysis (Fig. 3) was conducted to obtain absolute molecular weights of the polymers. The molecular weights measured by MALDI-TOF analysis were consistent with M_n s based on the ¹H NMR analysis. The entire identified mass fraction, separated by the mass of repeating units, contained the mass of the initiator, confirming that PAES with a controlled number and length of arms was synthesized without self-polymerization. Characterization details of the polymers are summarized in Table 1.

Thermal properties and viscosities

Thermal properties of the synthesized polymers were studied by DSC. Fig. 4 shows thermograms of the polymers recorded during the 2nd heating cycle at the heating rate of 5 °C min⁻¹ in a nitrogen atmosphere.

All the polymers exhibited glass transition temperature (T_g) between 150 °C and 180 °C which was strongly dependent on the molecular weight as well as the architecture. According to Ueberreiter and Kanig, the inverse of the T_g can be expressed as



Scheme 2 Synthesis of PAESs initiated from **1A**, **2A**, **3A**, and **4A** initiator.

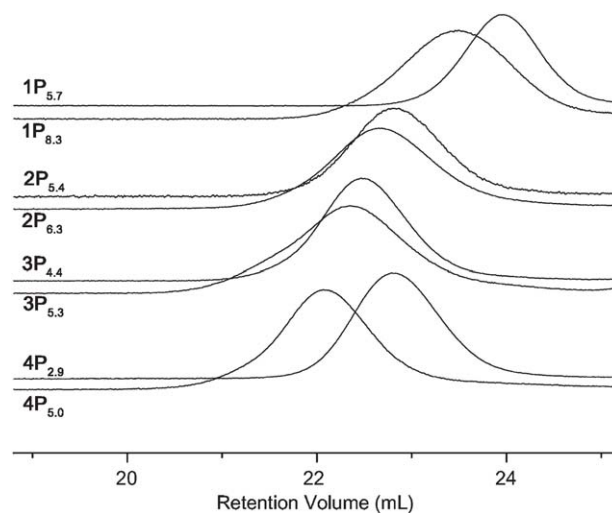


Fig. 1 THF-GPC profiles of synthesized polymers (RI detector).

a function of the inverse of M_n as shown in eqn (1), considering a polymer as a copolymer of internal units and end groups.³⁰ Eqn (1) includes Fox–Flory relation as an approximation limited to higher molecular weight polymers where the weight fraction of the end groups is small.^{31,32}

$$\frac{1}{T_g} = \frac{1}{T_{g\infty}} + \frac{K'}{M_n} \quad (1)$$

Roovers and Toporowski accounted the effect of the number of arms in the cases of star-shaped polymers by multiplying the number of arms (A) to K' because the inverse of M_n can be considered as the concentration of the end groups (eqn (2)).³³ In Fig. 5, the inverse of T_g is plotted against the number of ends (*i.e.*, end groups) per molecule divided by M_n (NMR), which should be proportional to the volume concentration of end groups in the polymer.

$$\frac{1}{T_g} = \frac{1}{T_{g\infty}} + \frac{K'A}{M_n} \quad (2)$$

Contradictory to Roovers' results where the identical trend was found for four-/six-arm star-shaped and linear polystyrenes, Fig. 5 showed a distinct difference between the linear polymers

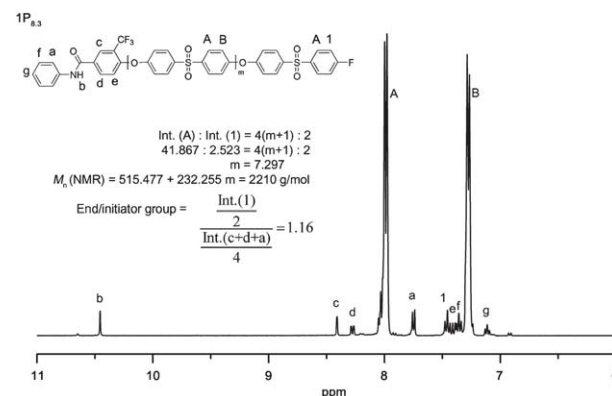


Fig. 2 ¹H NMR spectrum of **1P**_{8.3} (DMSO-*d*₆, 400 MHz).

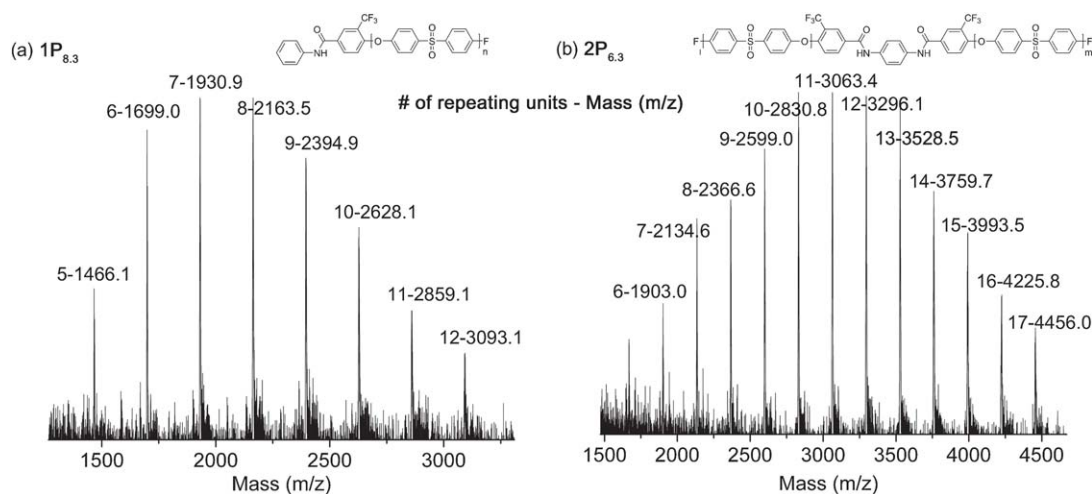


Fig. 3 MALDI-TOF mass spectra of (a) $1P_{8.3}$ and (b) $2P_{6.3}$.

($1P$ and $2P$) and the star-shaped polymers ($3P$ and $4P$). While $1P$ s have the $T_{g\infty}$ and K' values same as $2P$ s due to the linear architecture, $3P$ s and $4P$ s have different values. Star-shaped polymers ($3P$ and $4P$) possessed higher T_g when they had the identical concentration of end groups (*i.e.*, DP per arm). This effect was attributed to the presence of the central branch point in the star-shaped polymers which encumbers the segmental motion as pointed out by Meares and Bywater.^{34,35} This architecture-dependent effect was detectable because the polymers used in this study had lower molecular weights compared to Roovers' study and therefore the weight fraction of the central branch points/end groups was significant.

These architectural differences of the polymers also affected the viscosities of polymer solutions. Intrinsic viscosities of the polymer solutions were measured in DMF using Ubbelohde viscometer (Table 1). It is obvious that polymer with higher M_n possessed higher $[\eta]$ because of larger hydrodynamic volume. However, it is also observed that introduction of a central branch point decreased $[\eta]$ by reducing the hydrodynamic volume when the molecular weights of the polymers were similar. It can be quantitatively accounted by introducing the branching factor (g') which is calculated by dividing the intrinsic viscosities of a branched polymer by that of a linear one with the same molecular weight. For the polymers with M_n of ~ 3500 g mol⁻¹ in this study, g' of $3P_{4.4}$ was estimated as 0.93 and that of $4P_{2.9}$ as

0.72, when $2P_{6.3}$ was used as a linear reference. Again, these values clearly show the effect of the branching architecture on the physical properties of the polymer.

Physical gelation in THF

Conventional poly(arylene ether sulfone)s are usually soluble in methylene chloride and polar aprotic solvents such as NMP and DMF, while insoluble in THF.³⁶ However, the polymers synthesized in this study *via* CGCP showed fairly good solubility in THF. Even it was possible to make 10 g L⁻¹ solutions except for $1P_{8.3}$, of which the maximum solubility was less than 10 g L⁻¹ even at elevated temperature. However, the transparent solutions in THF (10 g L⁻¹) gradually turned into milky gels at room temperature, except $3P_{4.4}$ and $4P_{2.9}$ (Fig. 6a). Gelation occurred within 10 minutes in the cases of $1P_{5.7}$, $2P_{5.4}$, and $2P_{6.3}$, while it took several hours for $3P_{5.3}$ and $4P_{5.0}$. These gels were stable at room temperature but became sol again upon heating. The transition was fully reversible showing no indication of decomposition, after a number of cycles of heating and cooling.

Field-emission scanning electron microscopy (FE-SEM) showed that the gel was composed of a dense network of fibers with diameters ranging from 10 to 100 nm which immobilized THF inside (Fig. 6b–f), while THF-soluble $3P_{4.4}$ and $4P_{2.9}$ did not produce such a morphology (Fig. 6g). No notable differences

Table 1 Polymerization results, molecular weights, and physical properties

Entry	No. of arms	DP per arm (NMR) ^a	M_n (NMR) ^a	M_n (GPC) ^b	PDI ^b	M_n (GPC)/ M_n (NMR)	T_g ^c	$[\eta]$ ^d /cm ³ g ⁻¹
$1P_{5.7}$	1	5.7	1610	2270	1.08	1.41	151	5.4
$1P_{8.3}$	1	8.3	2210	2950	1.18	1.33	164	6.3
$2P_{5.4}$	2	5.4	2940	4440	1.14	1.51	173	10.9
$2P_{6.3}$	2	6.3	3400	4750	1.20	1.40	177	12.0
$3P_{4.4}$	3	4.4	3730	5550	1.15	1.49	177	11.2
$3P_{5.3}$	3	5.3	4370	5750	1.30	1.32	185	12.2
$4P_{2.9}$	4	2.9	3580	4440	1.12	1.24	165	8.6
$4P_{5.0}$	4	5.0	5570	6740	1.26	1.21	179	12.9

^a On the basis of the integration of ¹H NMR spectra of polymers. ^b Determined by THF-GPC using polystyrene standards (RI detector). ^c Measured by DSC with a heating rate of 5 °C min⁻¹ (2nd scan). ^d Intrinsic viscosity, measured in DMF at 30.5 °C.

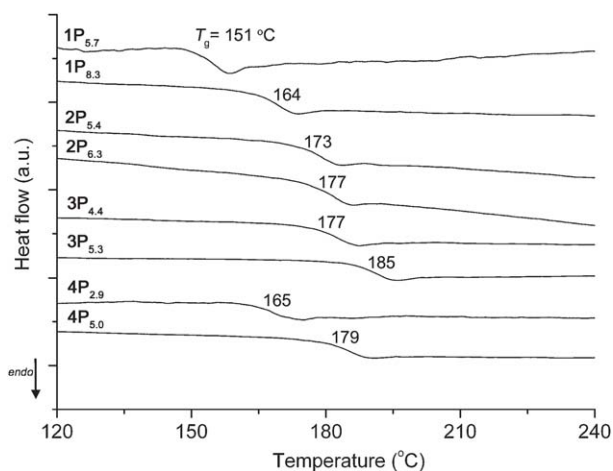


Fig. 4 DSC thermograms of the polymer (2nd heating scan with the heating rate of 5 °C min⁻¹ in N₂).

were observed between the polymers having different numbers of arms. Fig. 6h and i show electron micrographs of **2P_{6.3}** gel obtained with a field-emission transmission electron microscope (FE-TEM), indicating the amorphous nature of the fibers.

The solubility of the polymers was tested in other solvents, including *n*-hexane, ethanol, ethyl acetate, methyl ethyl ketone, acetonitrile, acetone, 1,4-dioxane, methylene chloride, chloroform, ethylene dichloride, toluene, chlorobenzene, and *o*-dichlorobenzene. As expected, the polymers showed good solubility in chlorinated aliphatic solvents and moderate solubility in acetone but were insoluble in other solvents.

Table 2 summarizes the gelation behavior of the polymer in THF. It turned out that the number of repeating units per arm, not the number of repeating units per polymer, was critical in the formation of gel. The polymers having approximately 5 repeating units per arm formed a gel regardless of the number of arms. The polymers with repeating units less than 5 per arm were soluble in THF and did not form a gel. If the number of repeating

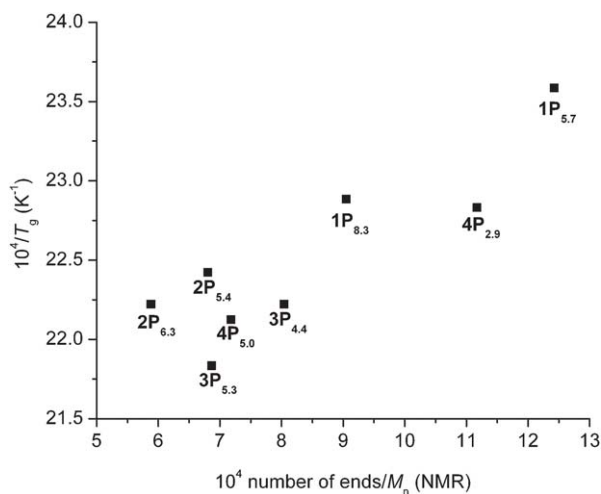


Fig. 5 Dependence of glass transition temperature on the number of end groups per molecule divided by the molecular weight of the polymer, *i.e.*, the end group concentration in the sample.

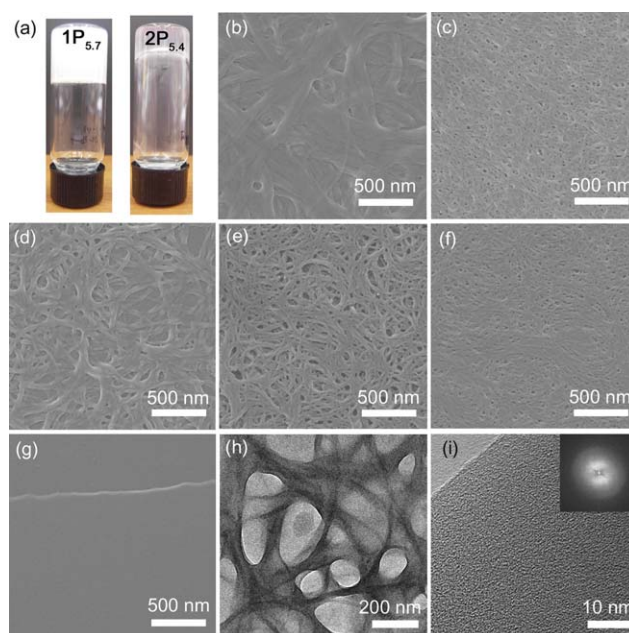


Fig. 6 (a) Optical image of **1P_{5.7}** gel (left) and **2P_{5.4}** gel (right). FE-SEM images of the xerogel of (b) **1P_{5.7}**, (c) **2P_{5.4}**, (d) **2P_{6.3}**, (e) **3P_{5.3}**, (f) **4P_{5.0}**, and dried sol of (g) **4P_{2.9}**. FE-TEM images of the xerogel of (h) **2P_{6.3}**, and (i) a magnified fiber of **2P_{6.3}** in high resolution mode (inset: FFT image).

units per arm were much greater than 5 (*i.e.*, **1P_{8.3}**), the polymer became insoluble in THF like conventional PAES. These solubility properties suggest that the unusual solubility of PAES synthesized in this study originates from the end groups and initiating moiety of the polymers. Because the molecular weights of the polymers are quite low, both the end groups and the initiating moiety occupy significant fractions. Especially the initiating moiety should play an important role since it contains aromatic secondary amides and trifluoromethyl groups which enhance the solubility in THF. Based on the group solubility approximation, relative energy difference (RED) value of PAES in THF was 1.237, indicating that PAES would be insoluble.³⁶ The existence of aromatic secondary amides and trifluoromethyl groups seems to decrease the RED value. If the number of repeating units is less than 5, it is expected that the RED value will be less than 1, making the polymer soluble in THF. As the number of repeating units per arm increases, the relative fraction of the initiating moiety decreases compared to the repeating unit and the enhancement on the solubility in THF should become insignificant.

It seems that the initiating moiety played an important role not only in the enhancement of solubility in THF, but also in the gelation by forming hydrogen bonds between the amides. Temperature-dependent ¹H NMR spectroscopy experiments were conducted for **2P_{6.3}** and **4P_{2.9}** in THF-*d*₈ to investigate the role of hydrogen bonding. Fig. 7a illustrates ¹H NMR spectra of **2P_{6.3}** in THF-*d*₈ (10 g L⁻¹) recorded at 27 °C (gel state) and 60 °C (sol state). When the temperature increased, the peak corresponding to the amide proton shifted from 9.6 ppm to 9.3 ppm ($\Delta = 0.27$ ppm), indicating the disruption of hydrogen bonds between the amides at elevated temperature. Compared to that, the solution of **4P_{2.9}** in THF-*d*₈ (10 g L⁻¹) maintained its sol state

Table 2 Gelation of polymers in THF (10 g L⁻¹)

Entry	1P _{5,7}	1P _{8,3}	2P _{5,4}	2P _{6,3}	3P _{4,4}	3P _{5,3}	4P _{2,9}	4P _{5,0}
State ^a	G (3.4) ^b	I	G (4.7)	G (4.5)	S	G (9)	S	G (10)

^a G: Gel, S: soluble, and I: insoluble. ^b In parentheses: CGC (g L⁻¹).

at 27 °C as well as at 60 °C, and the extent of the upfield shift of the peak corresponding to the amide proton was smaller ($\Delta = 0.17$ ppm) than that of 2P_{6,3} solution.

FT-IR measurements of the polymer solutions in THF also support the importance of hydrogen bonding in gelation. Fig. 8a shows the amide I and amide II vibrational bands of 2P_{6,3} in the gel and the sol state, respectively. When the solution became gel upon cooling, the bands showed large red-shift, clearly indicating the formation of hydrogen bonds. The intensity of hydrogen bonding of 3P_{5,3} was relatively weak reflected in the small red-shift of the amide I and amide II vibrational bands when sol to gel transition occurred (shown in Fig. S2[†]). The polymer 4P_{2,9} did not show any shift of the amide absorption band as it did not show a sol-gel transition.

Taking the evidence together, we propose that gelation of the polymer solution (THF) is mainly driven by the aromatic amide motif at the initiating site which forms hydrogen bonding upon

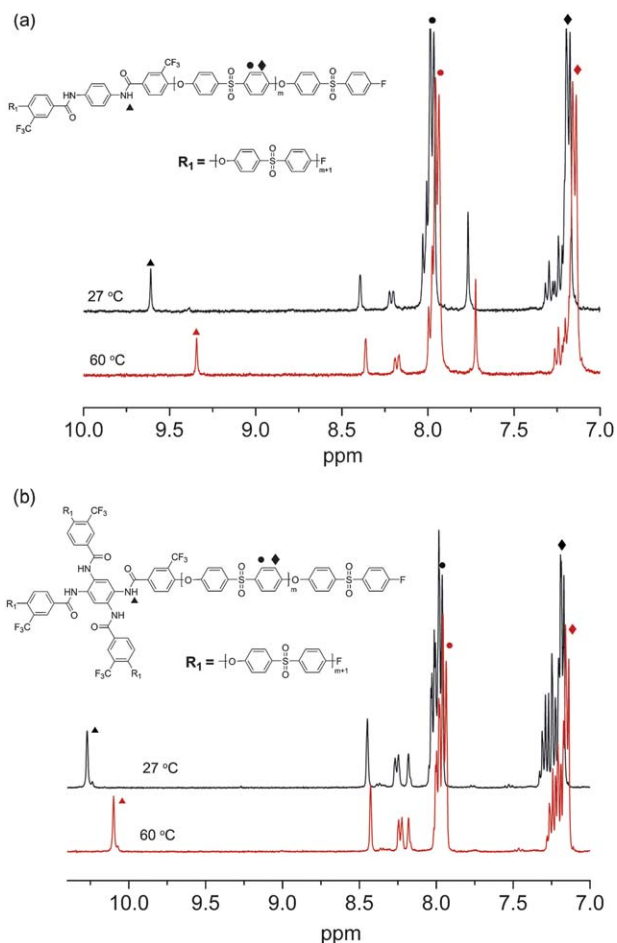


Fig. 7 Temperature-dependent ¹H NMR spectra of (a) 2P_{6,3} and (b) 4P_{2,9} (THF-*d*₈, 400 MHz) at 27, and 60 °C.

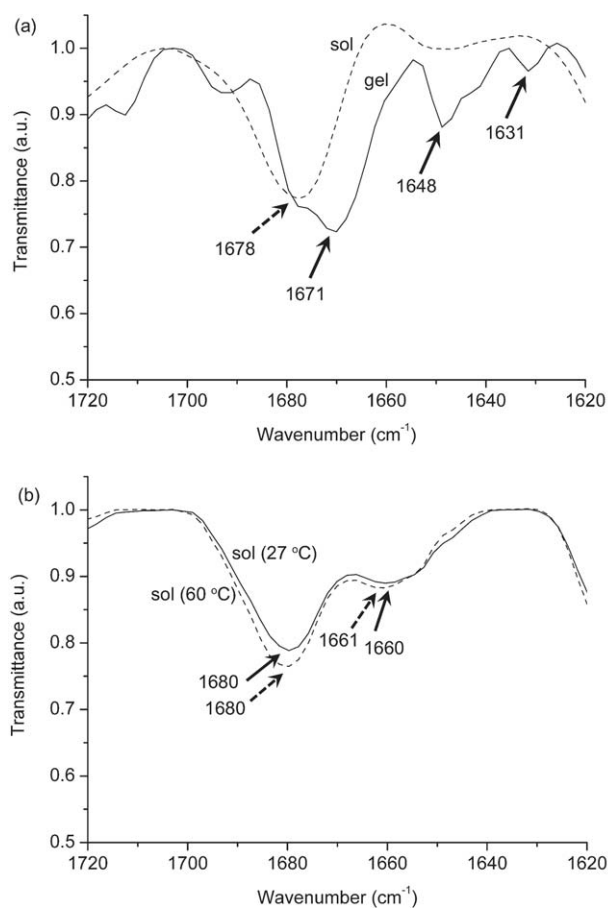


Fig. 8 FT-IR spectra of the (a) 2P_{6,3} and (b) 4P_{2,9} (10 g L⁻¹, THF).

cooling and produces self-assembled nanofibers. It seems that the stability of the gel comes from the effective protection of the hydrogen bonds by surrounded PAES chains which are solvophobic in THF, hence prevents THF molecules from the access to the amide. The suggested mechanism resembles to those proposed for low-molecular weight organogelators^{37–41} rather than polymers,^{42–45} which can be understood considering

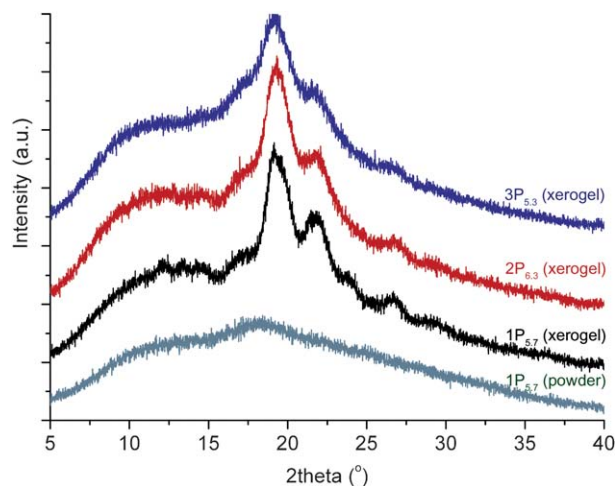


Fig. 9 Wide-angle powder XRD patterns of the polymers.

well-defined but rather low molecular weight of the polymers used in this study.

Powder X-ray diffraction patterns of the xerogels shown in Fig. 9 also support the above explanation. Because the PAES itself is amorphous,^{46,47} the as-synthesized **1P**_{5,7} did not show any diffraction. However, xerogel of the polymers showed peaks at the region of 18–30° which can be attributed to the structural periodicity of hydrogen bonded aromatic amides. It is also noted that **1P**_{5,7} and **2P**_{6,3} showed the peaks with relatively higher intensities compared to **3P**_{5,3}. It is speculated that the aromatic amides are more crowded as the number of arms connected to the initiator increases and the hydrogen bonds between the amides become weaker. These results are also found in the critical gelation concentration (CGC) of the polymers shown in Table 2, showing higher CGC for polymers with more number of arms.

Conclusions

Well-defined poly(arylene ether sulfone)s with various numbers of arms were successfully synthesized from multi-arm amide initiators (**1A–4A**) via chain-growth condensation polymerization. The physical properties of the polymers including T_g and viscosity were strongly affected not only by the molecular weight but also by the polymer architecture. Unexpected physical gelation of the polymer solutions attributed to the self-assembly of the polymers induced by the hydrogen bonding between the aromatic amides at the initiating moiety.

Acknowledgements

This work was supported by the National Research Foundation (NRF) through NRL (R0A-2008-000-20121-0) program, the Ministry of Environment through Contract No. 20090192091001-B0-0-001-0-0-2009, and Fundamental R&D program for Core Technology of Materials funded by the Ministry of Knowledge Economy, Republic of Korea.

References

- N. Hadjichristidis, M. Pitsikalis, S. Pispas and H. Iatrou, *Chem. Rev.*, 2001, **101**, 3747–3792.
- J. Pyun, X. Z. Zhou, E. Drockenmuller and C. J. Hawker, *J. Mater. Chem.*, 2003, **13**, 2653–2660.
- Y. Yagci and M. A. Tasdelen, *Prog. Polym. Sci.*, 2006, **31**, 1133–1170.
- K. Sada, M. Takeuchi, N. Fujita, M. Numata and S. Shinkai, *Chem. Soc. Rev.*, 2007, **36**, 415–435.
- D. Fournier, R. Hoogenboom and U. S. Schubert, *Chem. Soc. Rev.*, 2007, **36**, 1369–1380.
- S. S. Sheiko, B. S. Sumerlin and K. Matyjaszewski, *Prog. Polym. Sci.*, 2008, **33**, 759–785.
- C. L. McCormick, B. S. Sumerlin, B. S. Lokitz and J. E. Stempka, *Soft Matter*, 2008, **4**, 1760–1773.
- M. E. Fox, F. C. Szoka and J. M. J. Frechet, *Acc. Chem. Res.*, 2009, **42**, 1141–1151.
- J. Ueda, M. Kamigaito and M. Sawamoto, *Macromolecules*, 1998, **31**, 6762–6768.
- S. Angot, K. S. Murthy, D. Taton and Y. Gnanou, *Macromolecules*, 1998, **31**, 7218–7225.

- E. S. Kim, B. C. Kim and S. H. Kim, *J. Polym. Sci., Part B: Polym. Phys.*, 2004, **42**, 939–946.
- M. Trollsas and J. L. Hedrick, *J. Am. Chem. Soc.*, 1998, **120**, 4644–4651.
- K. Matyjaszewski, *Polym. Int.*, 2003, **52**, 1559–1565.
- R. Matmour, A. Lebreton, C. Tsitsilianis, I. Kallitsis, V. Heroguez and Y. Gnanou, *Angew. Chem., Int. Ed.*, 2005, **44**, 284–287.
- Z. S. Ge, J. Xu, J. M. Hu, Y. F. Zhang and S. Y. Liu, *Soft Matter*, 2009, **5**, 3932–3939.
- T. Yokozawa and A. Yokoyama, *Prog. Polym. Sci.*, 2007, **32**, 147–172.
- Y. J. Kim, M. Seo and S. Y. Kim, *J. Polym. Sci., Part A: Polym. Chem.*, 2010, **48**, 1049–1057.
- R. Sugi, Y. Hitaka, A. Yokoyama and T. Yokozawa, *Macromolecules*, 2005, **38**, 5526–5531.
- K. Yoshino, A. Yokoyama and T. Yokozawa, *J. Polym. Sci., Part A: Polym. Chem.*, 2009, **47**, 6328–6332.
- J. B. Rose, *Polymer*, 1974, **15**, 456–465.
- J. Park, M. Moon, M. Seo, H. Choi and S. Y. Kim, *Macromolecules*, 2010, **43**, 8304–8313.
- H.-H. Lin and Y.-L. Cheng, *Macromolecules*, 2001, **34**, 3710–3715.
- B. Loppinet, E. Stiakakis, D. Vlassopoulos, G. Fytas and J. Roovers, *Macromolecules*, 2001, **34**, 8216–8223.
- D. Vlassopoulos, *J. Polym. Sci., Part B: Polym. Phys.*, 2004, **42**, 2931–2941.
- S. J. Lee, B. R. Han, S. Y. Park, D. K. Han and S. C. Kim, *J. Polym. Sci., Part A: Polym. Chem.*, 2006, **44**, 888–899.
- K. Nagahama, T. Ouchi and Y. Ohya, *Adv. Funct. Mater.*, 2008, **18**, 1220–1231.
- F. van de Manacker, T. Vermonden, N. el Morabit, C. F. van Nostrum and W. E. Hennink, *Langmuir*, 2008, **24**, 12559–12567.
- N. Stavrouli, A. Kyriazis and C. Tsitsilianis, *Macromol. Chem. Phys.*, 2008, **209**, 2241–2247.
- T. Yokozawa, T. Taniguchi, Y. Suzuki and A. Yokoyama, *J. Polym. Sci., Part A: Polym. Chem.*, 2002, **40**, 3460–3464.
- K. Ueberreiter and G. Kanig, *J. Colloid Sci.*, 1952, **7**, 569.
- T. G. Fox and P. J. Flory, *J. Appl. Phys.*, 1950, **21**, 581.
- T. G. Fox and P. J. Flory, *J. Polym. Sci.*, 1954, **14**, 315.
- J. E. L. Roovers and P. M. Toporowski, *J. Appl. Polym. Sci.*, 1974, **18**, 1685–1691.
- P. Meares, in *POLYMERS: Structure and Bulk Properties*, Van Nostrand Reinhold Company, London, 1965, ch. 10.
- S. Bywater, *Adv. Polym. Sci.*, 1979, **30**, 89–116.
- C. M. Hansen, in *Hansen Solubility Parameters: a User's Handbook*, CRC Press, Boca Raton, 2nd edn, 2007, ch. 5.
- U. Beginn, S. Sheiko and M. Moller, *Macromol. Chem. Phys.*, 2000, **201**, 1008–1015.
- J. J. van Gorp, J. Vekemans and E. W. Meijer, *J. Am. Chem. Soc.*, 2002, **124**, 14759–14769.
- M. Suzuki, Y. Nakajima, M. Yumoto, M. Kimura, H. Shirai and K. Hanabusa, *Langmuir*, 2003, **19**, 8622–8624.
- C. C. Xue, S. Jin, X. Weng, J. J. Ge, Z. H. Shen, H. Shen, M. J. Graham, K. U. Jeong, H. B. Huang, D. Zhang, M. M. Guo, F. W. Harris, S. Z. D. Cheng, C. Y. Li and L. Zhu, *Chem. Mater.*, 2004, **16**, 1014–1025.
- J. Puigmarti-Luis, A. Minoia, A. P. del Pino, G. Ujaque, C. Rovira, A. Lledos, R. Lazzaroni and D. B. Amabilino, *Chem.–Eur. J.*, 2006, **12**, 9161–9175.
- S.-k. Ahn, R. M. Kasi, S.-C. Kim, N. Sharma and Y. Zhou, *Soft Matter*, 2008, **4**, 1151–1157.
- C. Tsitsilianis, *Soft Matter*, 2010, **6**, 2372–2388.
- M. Suzuki and K. Hanabusa, *Chem. Soc. Rev.*, 2010, **39**, 455–463.
- D. Ka, M. Seo, H. Choi, E. H. Kim and S. Y. Kim, *Chem. Commun.*, 2010, **46**, 5722–5724.
- F. Lufrano, G. Squadrato, A. Patti and E. Passalacqua, *J. Appl. Polym. Sci.*, 2000, **77**, 1250–1256.
- R. Guan, H. Zou, D. P. Lu, C. L. Gong and Y. F. Liu, *Eur. Polym. J.*, 2005, **41**, 1554–1560.